


# openheart Novel approach to artefact detection and the definition of normal ranges of segmental strain and strain-rate values

Mikhail Kornev,<sup>1,2</sup> Hatice Akay Caglayan,<sup>1,2</sup> Alexander Kudryavtsev,<sup>1,3</sup> Sofia Malyutina,<sup>4,5</sup> Andrew Ryabikov ,<sup>4,5</sup> Michael Styliadis,<sup>6</sup> Henrik Schirmer ,<sup>7</sup> Assami Rösner <sup>1,2</sup>

**To cite:** Kornev M, Caglayan HA, Kudryavtsev A, *et al.* Novel approach to artefact detection and the definition of normal ranges of segmental strain and strain-rate values. *Open Heart* 2022;**9**:e002136. doi:10.1136/openhrt-2022-002136

Received 12 September 2022  
Accepted 28 November 2022

## ABSTRACT

**Aims** Strain artefacts are known to hamper the correct interpretation of segmental strain and strain-rate (S/SR). Defining the normal ranges of myocardial segmental deformation is important in clinical studies and routine echocardiographic practice. In order to define artefact-free normal ranges for segmental longitudinal S/SR parameters, we investigated the extent to which different types of artefacts and their segmental localisation in the three different myocardial layers created a bias in the results of echocardiographic strain measurements.

**Methods** The study included echocardiograms from men and women aged 40–69 years from two population-based studies, namely the Know Your Heart study (Russia) and the Tromsø Study (Norway). Of the 2207 individuals from these studies, 840 had normal results, defined as the absence of hypertension or indicators of any cardiovascular disease. Two-dimensional (2D) global and segmental S/SR of the three myocardial layers were analysed using speckle tracking echocardiography. Artefacts were assessed with two different methods: visual identification of image-artefacts and a novel conceptual approach of ‘curve-artefacts’ or unphysiological strain-curve formation.

**Results** Segmental strain values were found to have significantly reduced in the presence of strain-curve artefacts ( $14.9\% \pm 5.8\%$  towards  $-20.7\% \pm 4.9\%$ ), and increased with the foreshortening of the 2D image. However, the individual global strain values were not substantially altered by discarding segmental artefacts. Reduction due to artefacts was observed in all segments, layers, systolic and diastolic strain, and SR. Thus, we presented normal ranges for basal-septal, basal, medial and apical segment groups after excluding artefacts.

**Conclusion** Strain-curve artefacts introduce systematic errors, resulting in reduced segmental S/SR values. In terms of artefact-robust global longitudinal strain, the detection of curve-artefacts is crucial for the correct interpretation of segmental S/SR patterns. Intersegmental S/SR gradients and artefacts need to be considered for the correct definition of normalcy and pathology.

## INTRODUCTION

Two-dimensional speckle tracking echocardiography (2DSTE) can be performed to

### WHAT IS ALREADY KNOWN ON THIS TOPIC

⇒ Artefacts are a major challenge in two-dimensional strain rate imaging.

### WHAT THIS STUDY ADDS

⇒ A novel method for strain artefact detection is proposed in this paper. Segmental strain and strain rate values are reduced in the presence of artefacts. Segmental strain-curve artefacts do not affect global strain significantly.

### HOW THIS STUDY MIGHT AFFECT RESEARCH, PRACTICE OR POLICY

⇒ The new approach of artefact detection might become a useful addition to automated and real-life speckle tracking. We provide artefact-free layer specific reference values for segmental strain and strain rate.

assess global and regional strains, strain-rate (SR) curves, as well as peak values in different ventricles, layers and dimensions. Among these, global longitudinal strain (GLS) is most frequently used due to its robustness and higher specificity in revealing latent systolic dysfunction than ejection fraction (EF).<sup>1</sup>

Segmental strain patterns can indicate subtle regional pathologies in patients with different types of myocardial and cardiovascular diseases (CVD).<sup>2</sup> The assessment of regional myocardial function using 2DSTE remains a challenge in clinical cardiology,<sup>3</sup> due to poor reproducibility caused by factors such as tracking algorithms, poor image quality and image artefacts.<sup>4,5</sup> Furthermore, strain-curve artefacts may lead to the misinterpretation of regional pathologies, causing lower reproducibility, especially for segmental S/SR and the strains of three myocardial layers,<sup>3,4,6–9</sup> affecting the normalcy<sup>7,10,11</sup> and pathology of the heart. Furthermore, the artificial segmental strain might cover up subtle



© Author(s) (or their employer(s)) 2022. Re-use permitted under CC BY-NC. No commercial re-use. See rights and permissions. Published by BMJ.

For numbered affiliations see end of article.

### Correspondence to

Dr Assami Rösner; assami.rosner@unn.no

functional changes which might be present between age, sex or cardiovascular risk factors.

In this study, a novel approach for defining non-physiological strain curves, which are commonly observed in the presence of erroneous tracking and noise artefacts, has been proposed in the use of artefact detection in a population with normal cardiac function. The objectives of this study were to (1) correlate curve artefacts with 2D imaging artefacts; (2) describe the effects of curve artefacts on the S/SR values; (3) investigate whether discarding segments with curve artefacts changes the layer-specific segmental or global S/SR values; (4) investigate the dependency of S/SR values on cardiovascular-related risk factors, sex and age and (5) define normal references for layer-specific segmental strain as well as systolic and diastolic segmental SR.

## METHODS

### Study population

In this study, data were used from the seventh wave of the Norwegian Tromsø Study (Tromsø7) and the Russian Know Your Heart (KYH) Study conducted in Arkhangelsk and Novosibirsk, which were cross-sectional population health studies conducted in parallel between 2015 and 2018 with harmonised questionnaires and echocardiography protocols.

The study sample was randomly selected from all participants who underwent echocardiography (2340 from

Tromsø and 4521 from Russia), including 50% participants from Tromsø7, 25% from Arkhangelsk and 25% from Novosibirsk. The selection included three equal-sized age groups (40–49, 50–59 and 60–69 years). As shown in figures 1 and 2D, strain analysis was performed on 1194 and 1013 participants aged 40–69 years from the KYH and Tromsø7 studies, respectively.

### Data collection from KYH and Tromsø7 studies

Health checks included a medical examination, questionnaire and biological sample collection. Participants underwent transthoracic echocardiography using GE VividQ with a 1.5–3.6-MHz transducer in Russia and Vivid E9 with a 1.5–4.6-MHz matrix probe in Norway. 2D greyscale images and pulsed, continuous and colour Doppler data were acquired in the parasternal and apical views. Greyscale images were obtained at a frame rate of at least 50 fps. Images were analysed offline using the commercial software EchoPAC (V.203; GE-Vingmed AS, Horten, Norway). Trained echocardiography specialists performed examinations following standard operational procedures, and intraobserver and interobserver variabilities for conventional echocardiographic measures were regularly assessed within and between both Russian and Norwegian reading laboratories. Written informed consent for research and publication was obtained from all study participants.

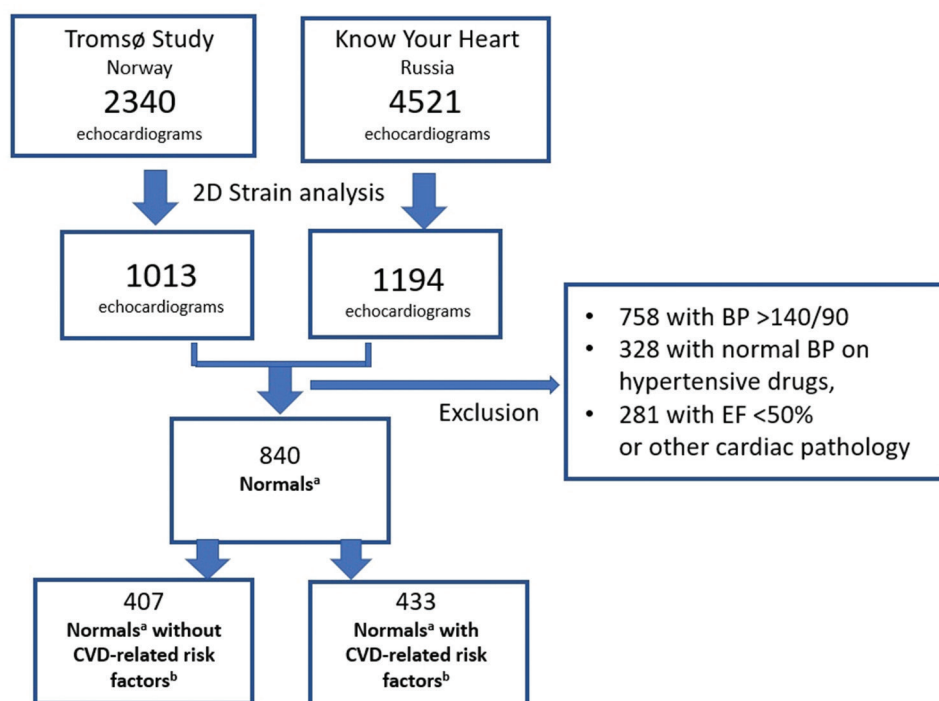


**Figure 1** Inclusion of participants and distribution into groups. Beyond high blood pressure (BP) and BP medication, participants were excluded when ejection fraction (EF) was reduced, when they had a history of a cardiac attack or other cardiac diseases, or when echocardiography showed cardiac pathology. <sup>a</sup>Participants with normal heart structure and functioning. <sup>b</sup>CVD-related risk factors used for group definition: increased low-density lipoprotein, increased HbA1C, high BMI or diabetes history. BMI, body mass index; CVD, cardiovascular disease.

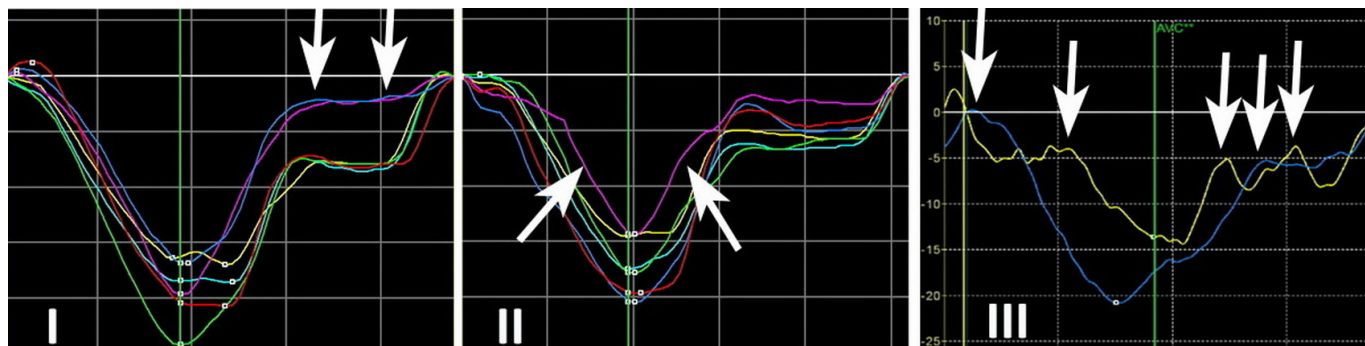


**Figure 2** Strain-curve artefacts: (I) ‘Diastolic mismatch’ artefact was defined when the late diastolic strain-curve strongly deviated from the late diastolic strain-curve of other segments (arrows). (II) ‘Blunted curves’ artefact was defined as a reduced or even positive strain at the start of the cycle (left arrow), mirrored by a similar curve formation at the end of systole (right arrow), and PSS was missing although ES strain was significantly lower than those for other segments. Presence of PSS is seen in the non-artificial yellow curve of the first panel. as a shortening of the segment after aortic valve closure (marked as the green line) (III) ‘Floating curves’ were defined as segmental strain curves with several negative and positive peaks without correspondence with timing or configuration of other segments (arrows mark peaks of the yellow curve without time-relation towards the blue curve). ES, end-systolic; PSS, post systolic shortening.

### Definition of healthy participants with normal left ventricular function

Healthy participants with normal left ventricular (LV) function were defined by excluding those who fulfilled the following criteria: Self-reported or ECG-detected atrial fibrillation; systolic blood pressure >140 mm Hg or diastolic blood pressure >90 mm Hg; and the self-reported use of antihypertensives, renin-angiotensin system agents, beta-blockers or calcium antagonists; EF <50%; aortic insufficiency grades 3–4; aortic valve mean pressure gradient >25 mm Hg; mitral insufficiency grades 3–4; moderate-grade and high-grade mitral stenosis; LV diameter >57 mm for women and >60 mm for men; Q-wave on ECG (classes 1.1–1.2.7. of Minnesota code); history of myocardial infarction or heart attack; left bundle branch block on ECG; increased NTpro-BNP according to clinical age-specific and sex-specific limits; peak tricuspid regurgitation gradient >30 mmHg.

### Definition of subgroups

Artefacts—average of segments versus GLS:

In one group, average end-systolic (ES) segmental curves or peak-SR were calculated after excluding segmental curve artefacts and foreshortening. In the other group, the same parameters, including artefacts, were averaged. For global S/SR, the peak global S/SR values were used as extracted by the software and then averaged for the values of the three different views.

### Cardiovascular risk factors

The population with normal conventional echocardiographic characteristics was divided into two groups—with and without these CVD-related risk factors<sup>12</sup>—to investigate the role of increased cholesterol, body mass index (BMI) or diabetes on strain values in a population-based study. Remarkably, smoking has not been reported as an independent factor associated with reduced strain and was, accordingly, not used for grouping based on risk factors. As previously mentioned, individuals with

hypertension were excluded from the study population due to their altered cardiac structure and function.

### Age and sex

S/SR values were investigated for dependency on age and sex to merge groups with and without risk factors, age and sex for the establishment of normal ranges if they were not significantly or marginally different.

### Strain and SR analysis

Data for strain measurements were obtained in apical two-chamber (2CH) and four-chamber (4CH) and apical long-axis (APLAX) echocardiographic views. The KYH study did not include APLAX images. All strain data were analysed using the Q-analysis function of EchoPAC. The myocardial borders were manually traced. When necessary, the automatically assigned time point of aortic valve closure (AVC) was manually corrected. ES segmental subendocardial (endo), mid-myocardial (myo) and subepicardial (epi) strain, peak systolic SR (SR-S), peak diastolic SR-E, SR at atrial contraction (SR-A) and respective global S/SR values were extracted. ES strain was selected as it is measured at the same time point and, thus, is more comparable to GLS. End-diastole was defined as the time point at peak R. End-systole was defined as the time point of AVC, which can be visualised by detecting the closure click using the spectral tracing of the pulsed-wave Doppler along the LV outflow tract. LV systole was measured from the peak of the R wave to AVC, and LV diastole was defined as the time between AVC and peak R.

The APLAX views of 176 Tromsø7 participants were analysed. In this subpopulation, the apical, medial, basal and basal-septal segments were analysed for differences to define groups of segments that displayed similar values.

### Artefact reading

Artefact detection was performed using screenshots of the strain curves generated by the EchoPAC software. We assessed the artefacts using two different methods.

The first method was the visual identification of image artefacts, mainly including noise artefacts, reverberations or missing parts of the myocardium. Apical foreshortening was subjectively assessed when the apical part of the ventricle had a round shape and showed downward motion during systole.

The second method, which has been introduced in this study, was the concept of ‘curve artefact’, defined as non-physiological strain-curve shapes. The concept of ‘curve artefact’ comprises three types of artefacts that are illustrated by typical strain curves (figure 2).

### Statistical analyses

Unless stated otherwise, continuous data are presented as mean±SD. Categorical characteristics are presented as absolute numbers and proportions. Between-group differences in continuous echocardiographic parameters were assessed using analysis of variance with Bonferroni post hoc tests. The  $\chi^2$  test was performed for group comparisons of categorical variables. Reference values were defined by the normal distribution describing mean values of  $\pm 1.96$  SD.

For intraobserver variability in S/SR measurements, 135 randomly selected echocardiographic records comprising 1620 segments were repeatedly analysed by the same observer 6–12 months after the initial analysis. To assess interobserver variability, the same images were reanalysed by a second observer trained in the same echocardiography laboratory. Both observers had performed at least 500 readings before reanalysis. Intraobserver and interobserver variabilities were assessed as limits of agreement derived from Bland-Altman plots with separate analyses for segments with and without curve artefacts. Statistical significance was set as a two-sided  $p < 0.05$ . SPSS V.26.0 (IBM) was used for statistical analyses.

## RESULTS

As shown in figure 1, this study included 840 healthy participants with normal heart structure and functioning out of the randomly selected 2207 participants. Table 1 presents the key demographic and health characteristics of the two groups with and without CVD-related risk factors. As expected, participants with CVD-related risk factors accounted for higher proportions of Russians; current smokers; and those with higher BMI, low-density lipoprotein cholesterol and glycosylated haemoglobin levels. There was no difference between the groups in blood pressure and LVEF, due to the exclusion of participants with hypertension and reduced EF from the normal population.

A comparison of S/SR between groups with and without CVD-related risk factors is presented in table 2. The epicardial strain increased from epicardial to endocardial values in both groups with and without CVD-related risk factors. There were no significant differences between the groups, except peak SR-A, which was higher in the group with CVD-related risk factors. Therefore,

**Table 1** Characteristics of the conditionally healthy population

	Normals* without CVD-related risk factors†	Normals* with CVD- related risk factors†	P value
	Mean ±SD or Abs (%)	Mean ±SD or Abs (%)	
<b>Total (participants)</b>	<b>407</b>	<b>433</b>	
Women	250 (61.4)	261 (60.3)	0.733
Men	157 (38.6)	172 (39.7)	
Russian	145 (35.6)	206 (47.6)	0.002
Norwegian	262 (64.4)	227 (52.4)	
Age (years)	53 ±8	53 ±8	0.571
BMI (kg/m <sup>2</sup> )	24.4 ±2.8	27.4 ±5.0	<0.001
Systolic BP (mm Hg)	118 ±12	119 ±13	0.303
Diastolic BP (mm Hg)	72 ±9	75 ±9	0.465
Total cholesterol (mmol/l)	5.0 ±0.6	6.1 ±1.1	<0.001
LDL cholesterol (mmol/l)	3.1 ±0.6	4.2 ±0.9	<0.001
HDL cholesterol (mmol/l)	1.7 ±0.4	1.5 ±0.5	0.212
HbA1C (%)	5.5 ±0.3	5.7 ±0.8	<0.001
Diabetes diagnosis	0	8 (2.1)	0.004
Smoking‡	68 (16.7)	97 (22.5)	0.036
LVEF (%)	58 ±5	57 ±5	0.572

\*Participants with normal heart structure and functioning.  
†CVD-related risk factors used for group definition: increased low-density lipoprotein, HbA1C, diabetes history, BMI.  
‡Refers to the active current smoking.  
.BMI, body mass index; BP, blood pressure; CVD, cardiovascular disease; HDL, high-density lipoprotein; LDL, low-density lipoprotein; LVEF, left ventricular ejection fraction.

we used merged groups with and without risk factors to define normal ranges.

### Influence of artefacts on segmental S/SR

Figure 3 shows the percentage of segments with either curve or noise artefacts or the presence of both curve and noise artefacts in the same segments. Of the 11 136 segments analysed, 1117 (10%) were assessed as curve artefacts, 794 (7.1%) as diastolic mismatch, 280 (2.5%) as blunted and 43 (0.4%) as floating curves. Some basal-septal and basal inferior segments displayed curve artefacts without noise artefacts, indicating other factors causing curve artefacts. The highest number of artefacts were found in the segments of the anterior and anterolateral walls. The percentage of segments with both types of artefacts was the highest when compared with that of segments with either curve or noise artefacts in all segments. Noise or other 2D image artefacts were present in 88% of curve artefacts, whereas all segments with noise artefacts displayed curve artefacts in 89%.

**Table 2** Strain and strain-rate in normal participants with and without CVD-related risk factors

	Normals* without CVD-related risk factors†	Normals* with CVD- related risk factors†	P value
	N=379	N=410	
	Mean ±SD	Mean ±SD	
ES-LS-epi (%)	-18.6 ±2.1	-18.4 ±2.2	0.247
ES-LS-myo (%)	-20.8 ±2.3	-20.6 ±2.5	0.266
ES-LS-endo (%)	-24.0 ±2.7	-23.8 ±3.1	0.414
Peak global SR-S (1/s)	-1.19 ±0.17	-1.20 ±0.18	0.454
Peak global SR-E (1/s)	1.67±0.33	1.64 ±0.32	0.196
Peak global SR-A (1/s)	1.03 ±0.24	1.08 ±0.25	0.009

\*Participants with normal heart structure and function.

†CVD-related risk factors used for group definition: increased low-density lipoprotein, HbA1C, diabetes history, BMI.

.CVD, cardiovascular disease; endo, endocardial; epi, epicardial; ES, end-systolic; LS, longitudinal strain; myo, myocardial; SR, strain-rate; SR-A, strain-rate at atrial contraction; SR-E, strain-rate at early diastole; SR-S, strain-rate at peak systole.

Thus, noise and curve artefacts most commonly exhibited imaging deficiencies, resulting in erroneous speckle tracking.

Figure 4 shows the myocardial strain values in different segments depending on the presence or absence of curve artefacts or foreshortened 2D projections. We found significantly reduced strain values in the presence of curve artefacts and increased strain values in the presence of foreshortening, which was present in 10.7% of all 2CH, and 20.2% of all 4CH views, and none in the group of 106 individuals with 3CH views.

### Effect of artefacts on global S/SR

Table 3 shows the influence of curve artefacts on the LV average or global S/SR values. Group A included average S/SR after discarding segmental artefacts. A lower N is due to discarding the results of images with foreshortening, which affected 4CH and 2CH views in 51 study participants. Group B included all segmental analyses, and group C displayed global S/SR. The global and segmental averaged strains, including segmental artefacts (groups B and C), were lower than the average segmental strain for all investigated S/SR parameters after artefacts were discarded (group A). Furthermore, the inclusion of curve artefacts led to a slight reduction in average S/SR. However, this reduction was less than the significantly greater GLS/SR reduction by curve artefacts. The average diastolic peak SR-E was not influenced by the presence of strain-curve artefacts. Figure 4 shows the range of the mid-myocardial strain in all segments. Comparing segmental S/SR values of 18 segments showed no significant differences between the segments of the basal-septal, basal, medial and apical groups ( $p>0.05$ ). Due to significant differences in S/SR between the basal-septal, basal, medial and apical segments, we decided to refer to the four segmental groups.

### Global S/SR based on age and sex

Figure 5 shows age and sex differences for S/SR parameters. The largest differences were found for peak-SR-A, which increased with age for each sex and was higher for women. There were also significant differences in peak-SR-E between the age groups and sex. Values for all S/SR parameters were higher for women and decreased with age for both men and women. No significant differences were observed between age groups for peak SR-S or segmental strain values, due to which normal reference

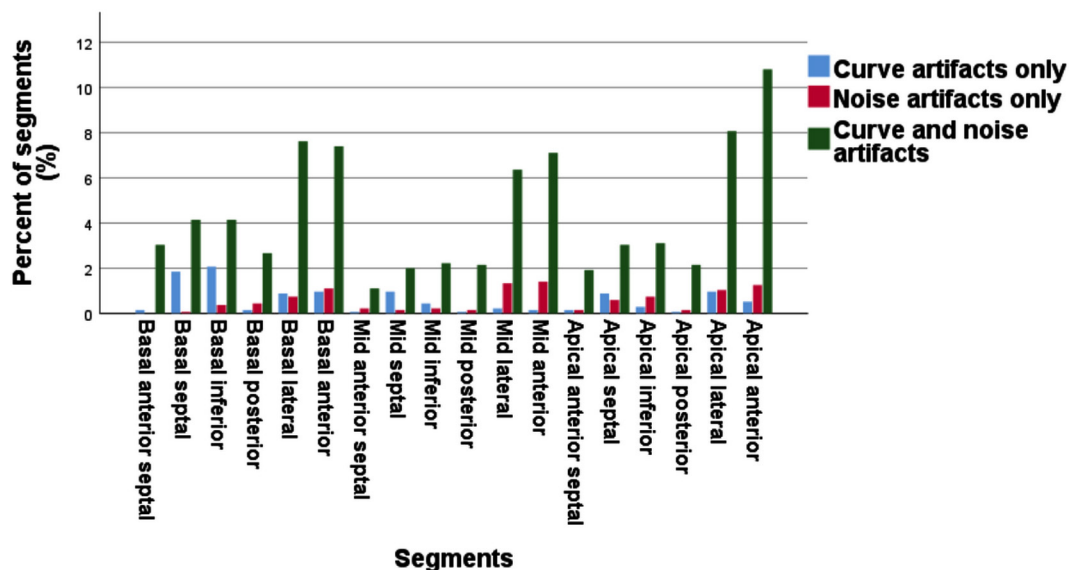


**Figure 3** Percentage of segments with either strain-curve artefacts or noise artefacts, or the presence of both curve and noise artefacts in the same segment.

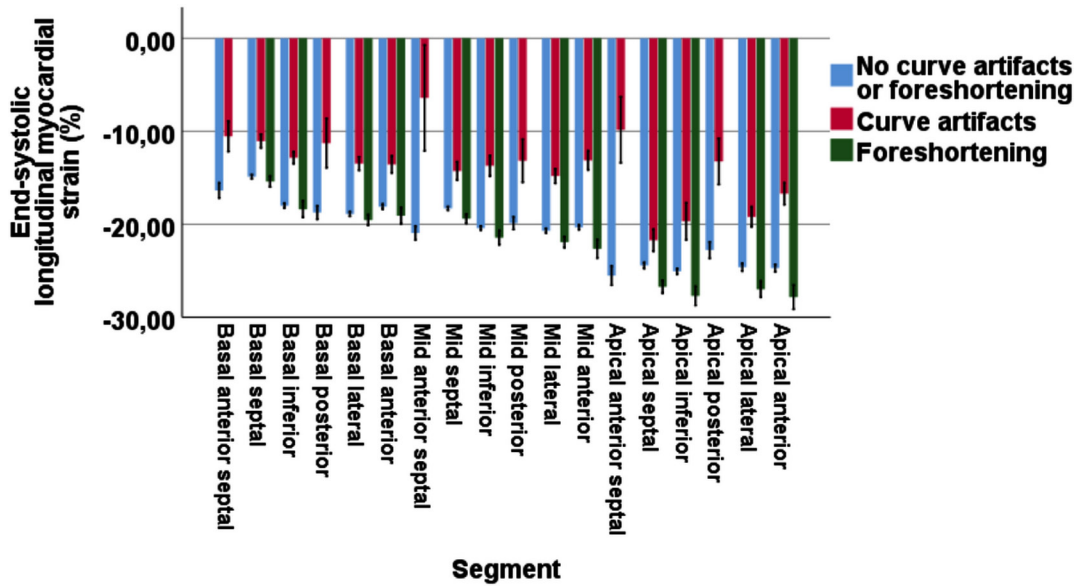


**Figure 4** Myocardial strain values in different segments depending on the presence or absence of curve artefacts or foreshortened 2D projections. 2D, two-dimensional.

S/SR values were not reported for the different age groups.

**Normal reference values**

Normal ranges for basal-septal, basal, medial and apical segments, excluding segments with artefacts, are presented in table 4. Owing to the significant differences between sexes, normal ranges are displayed separately for men and women. Each S/SR parameter showed a pattern

of gradual increase in the S/SR values from the basal to apical segmental groups. Strain values increased significantly from the epicardial to the endocardial position.

**Table 3** Influence of global strain and curve artefacts on strain and SR values

	Average of peak segmental values		Average of views
	Artefacts discarded (A) N=789	Artefacts included (B) N=840	Global Longitudinal Strain (C) N=840
	Mean ±SD	Mean ±SD	Mean ±SD
ES-LS-epi (%)	-18.5 ±2.2	-18.0 ±2.4*	-18.1 ±2.3*†
ES-LS-myo (%)	-20.7 ±2.4	-20.3 ±2.6*	-20.4 ±2.5*†
ES-LS-endo (%)	-23.9 ±2.9	-23.5 ±2.9*	-23.1 ±2.8*†
Peak-SR-S (1/s)	-1.20 ±0.18	-1.19 ±0.17*	-1.00 ±0.15*†
Peak-SR-E (1/s)	1.65 ±0.33	1.65 ±0.33	1.35 ±0.36*†
Peak-SR-A (1/s)	1.06 ±0.25	1.02 ±0.24*	0.86 ±0.20*†

Strain artefacts comprise artefacts identified by abnormal, ‘unphysiological’ strain curves or images of a foreshortened left ventricle.

\*p<0.05 for difference from group A.

†p<0.05 for difference from group B.

SR, strain-rate; ES, end-systolic; LS, longitudinal strain; epi, epicardial; myo, myocardial; endo, endocardial; SR-S, strain-rate at peak systole; SR-E, strain-rate at early diastole; SR-A, strain-rate at atrial contraction.; .

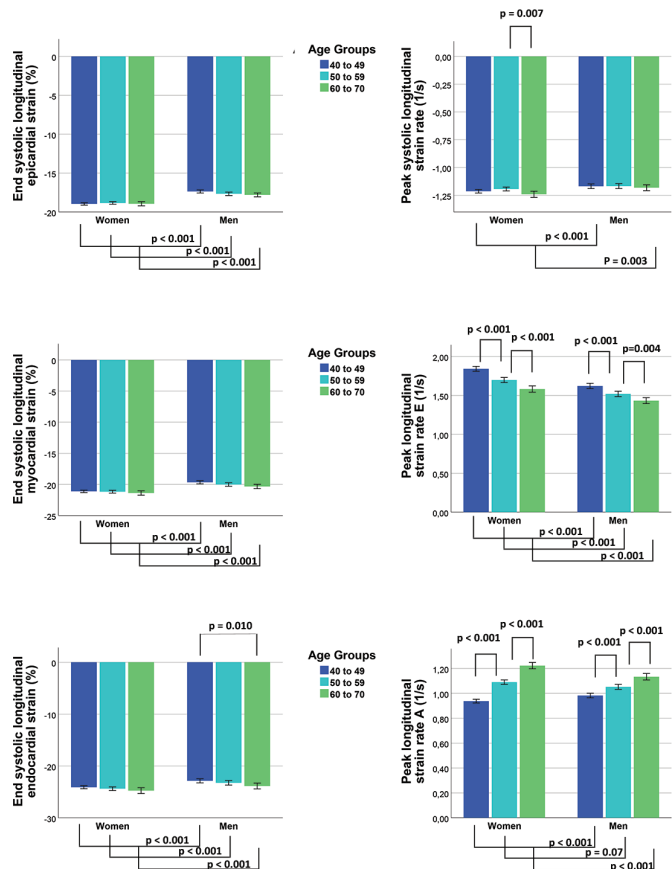


**Figure 5** Age and sex differences for S/SR parameters. S/SR, strain and strain-rate.

**Table 4** Normal ranges of segmental layer-specific strain and SR in ages from 40 to 69 years

	Basal-septal segments		Basal segments		Medial segments		Apical segments	
	Lower bound	Upper bound	Lower bound	Upper bound	Lower bound	Upper bound	Lower bound	Upper bound
<b>Women (N=479)</b>								
ES-LS-epi (%)	-9.1	-20.8	-13.4	-23.5	-15.4	-23.7	-13.4	-26.2
ES-LS-myo (%)	-9.5	-21.2	-14.0	-24.2	-16.2	-24.9	-17.2	-32.7
ES-LS-endo (%)	-9.4	-22.1	-14.3	-25.3	-17.0	-26.6	-22.5	-42.8
Peak-SR-S (1/s)	-0.52	-1.23	-0.70	-1.52	-0.80	-1.35	-0.82	-2.22
Peak-SR-E (1/s)	0.42	1.77	0.74	2.23	0.89	2.13	1.01	3.59
Peak-SR-A (1/s)	0.36	1.61	0.47	1.65	0.53	1.47	0.32	1.91
<b>Men (N=311)</b>								
ES-LS-epi (%)	-9.0	-19.2	-11.6	-21.5	-13.6	-22.5	-12.1	-25.4
ES-LS-myo (%)	-9.4	-19.6	-12.2	-22.1	-14.5	-23.9	-16.4	-31.7
ES-LS-endo (%)	-9.2	-20.7	-12.6	-23.1	-15.3	-25.8	-22.1	-41.4
Peak-SR-S (1/s)	-0.50	-1.16	-0.66	-1.36	-0.75	-1.32	-0.84	-2.17
Peak-SR-E (1/s)	0.46	1.68	0.70	2.04	0.74	1.83	0.94	3.04
Peak-SR-A (1/s)	0.46	1.56	0.50	1.54	0.59	1.43	0.47	1.81

endo, endocardial; epi, epicardial; ES, end-systolic; LS, longitudinal strain; myo, myocardial; SR, strain-rate; SR-A, strain-rate at atrial contraction; SR-E, strain-rate at early diastole; SR-S, strain-rate at peak systole.

### Reproducibility

Bland-Altman plots for inter- and intraobserver variabilities for the S/SR parameters are presented in online supplemental figures 1 and 2, respectively. Strain-curve artefacts had high reproducibility, displayed lower strain values and generated a systematic error with unexpectedly lower interobserver and intraobserver variabilities. Accordingly, higher variability was observed at higher strain values. However, the mean difference between the two readers, as well as repeated readings by the same investigator, were higher when artefacts were present.

### DISCUSSION

To the best of our knowledge, this is the first study to describe artefact recognition using a qualitative assessment of strain curves. The main findings were as follows: (1) The presence of curve artefacts matched the presence of noise or other 2D image artefacts in 88% of participants; (2) in the presence of curve artefacts, strain values were systematically reduced, and they were increased by foreshortened long-axis projections; (3) discarding strain-curve artefacts rendered segmental strains with higher mean values and lower variability, whereas global strain was not affected and (4) this study is the first to describe the artefact-free normal ranges for layer-specific segmental strain in a large randomly selected population with normal heart structure and function.

#### Methodological considerations in curve-artefact detection

Artefacts caused by errors in automatic tracking generally result in low peak strain and low SR results, leading to misinterpretation as false pathological results. The

concept of curve artefacts was built on the following considerations:

#### 'Diastolic mismatch'

Normal and pathological strain curves display distinct patterns, where systolic deformation patterns can change due to pathologies causing reduced or delayed regional or global systolic shortening. In contrast to the systolic and early diastolic strains, the late diastolic strain is expected to display uniform strain curves with parallel stretching patterns. At the time of maximal postsystolic shortening (when present), all segments reached a relaxed state at approximately equal segment lengths. After this time point, all segments stretch in parallel at the end of the early filling phase through diastasis of the ventricle and atrial contraction until reaching the initial segment length at end-diastole. As shown in figure 2-I, curves with deviating (often reduced) deformations of a single segment in late diastole can only represent an artefact. Thus, we called this type of artefact 'diastolic mismatch,' describing strong positive deviation of the late diastolic curve from the diastolic strain-curve of other segments.

#### 'Blunted curves'

Another curve-artefact type that was discovered could be caused by insufficient tracking at the beginning and end of the cardiac cycle. This type manifests as zero or positive initial strain, often mimicking the early onset of segmental stretching and the late onset of shortening. In the presence of true regional pathology, the strain of the segment with reduced contractility is significantly lower than the peak strain of the neighbouring segments, and the artefact-free curve displays post systolic shortening

(PSS). Delayed segmental shortening, early onset of segmental stretching before end-systole and missing PSS were the typical characteristics of a 'blunted' strain-curve.

#### 'Floating curves'

The third type of curve-artefact is associated with erroneous myocardial tracking, particularly when the myocardium is not being followed throughout the cardiac cycle. In this case, the strain curves do not follow a physiological pattern and show either oscillations or several positive and negative peaks without the corresponding peak strains of the neighbouring segments. In dyssynchrony or regionally reduced myocardial function, positive and negative peaks of the opposite segments can be displayed simultaneously. However, physiologically, the time points of positive and negative peaks in systole are simultaneous, and the peaks in diastole do not diverge after the time point of PSS. We defined 'floating curves' as present when several diverging positive and negative peaks were observed, and when the time points of onset or peak deviated from the onsets and peaks of all other segmental curves.

#### Influence of artefacts on segmental S/SR

Segmental curve artefacts appeared to be highly correlated with either the presence of artefacts in 2D images, such as noise and reverberations; thus, in most cases, curve and noise artefacts were observed together. This strengthens our hypothesis that a high proportion of 2D image artefacts produce curve phenomena. Most curve artefacts without 2D artefacts were from basolateral segments, where tracking is problematic because of lower lateral resolution. Segmental values with curve artefacts were significantly reduced for both strain and SR in all layers. According to our results, artefacts had a high impact on the segmental S/SR values. Thus, segmental curve artefacts need to be handled before drawing clinical conclusions from strain patterns on the segmental bullseye plot.

Apical foreshortening has already been described as a factor for the overestimation of strain values,<sup>13</sup> especially in the apical endocardium, which is consistent with the present findings. However, this overestimation probably does not apply to highly dysfunctional segments. The effect of foreshortening and curve-artefacts on clinical needs to be investigated in future studies.

#### Effect of artefacts on global S/SR

Discarding artefacts from the average strain calculation reduced the ES strain values by <0.5%. Average GLS and artefact-free strain differed by the same amount. Unexpectedly, subendocardial GLS was also lower than the segmental average with artefacts. This may be explained by a software algorithm that reduces the percentage of apical strain contribution to GLS, which affects endocardial GLS, with the highest apical to basal gradients. The difference between the segmental average of the LV and global values was even more noticeable for SR values.

The lower global longitudinal (GL) SR values than the average of segmental peaks are expected because the non-simultaneous time points of segmental peaks do not sum up to one blunted peak of the GL SR curve. Thus, when using SR-E as a clinical parameter, the average of peak values at different time points should be used. Although significant, the detection of segmental artefacts had little effect on GLS values and, accordingly, should not be considered when measuring GLS. To date, several studies on larger populations have suggested normal ranges for GLS or SR.<sup>1 12 14–18</sup> Accordingly, the normal ranges were integrated into the 2016 American Society of Echocardiography/European Association of Cardiovascular Imaging chamber quantification recommendations.<sup>12 19</sup> Our GLS results are in concordance with results of a recent meta-analysis,<sup>18</sup> where the mean normal values of mid-myocardial GLS varied from -15.9% to -22.1% (mean: 19.7%).

#### Global S/SR based on age and sex

Studies regarding the effects of age on LV longitudinal S/SR-A are limited. Therefore, the effect of age on LV myocardial deformation remains controversial. In this study, strain values were not significantly different between the age groups of 40 and 69 years, which is consistent with the findings of Nagata *et al.*<sup>11</sup> However, other studies reported a significant effect of ageing on systolic longitudinal myocardial velocities but not on the longitudinal S/SR,<sup>12 14 20</sup> which might be due to decreased systolic deformation from higher arterial stiffness with increasing vascular resistance and afterload. Accordingly, our results demonstrated a gradual decrease in SR-E and a gradual increase in SR-A with increasing age.

The lower global and segmental S/SR values in men than in women are consistent with those of previous studies.<sup>15 16 21–23</sup> Many features, such as lower systolic blood pressure; lower wall stress and afterload; and smaller body surface area, ventricular size and LV mass in women than in men, have favourable effects on LV systolic functional parameters. These composite factors seem to be a physiologically plausible reason for higher S/SR parameters in women than in men. Due to the significant differences in these factors between sex, we described the normal ranges separately for men and women.

#### Normal reference values

Only a small number of previous studies have yielded information regarding population-based normal segmental S/SR values.<sup>19 22 24 25</sup> Since segmental S/SR is highly affected by artefacts, the presented segmental systolic and diastolic layer S/SR ranges might serve well as a reference for segmental normalcy. Analysing strain by layers, a consistent gradient for segmental strains from the epi—towards the endocardial strain was found, which might explain the curvature of the ventricle, where the inner layer shortens as a sum of longitudinal shortening and radial displacement of the curved line towards the ventricular cavity.



LV segmental S/SR gradients with gradually increasing values from the basal to apical segments was also observed. The basal-apical gradients appear to be a physiological phenomenon, as they persisted after apical foreshortening, discarding artefacts and the exclusion of the hypertensive population.

### Limitations

This study has several limitations that must be acknowledged. First, the data in this study were obtained from a single reader and the ultrasound systems and software were provided by a single vendor. Therefore, strain variability may be substantially lower than with a multireader approach, which can be overcome with improvements in automated border detection. Second, the ages of the participants ranged from 40 to 69 years, indicating that the results cannot be extrapolated to older or younger participants. Third, although this study used data from two population studies conducted in different countries, the majority of participants were European Caucasians, indicating that the results should be extrapolated to other ethnic groups with caution. Fourth, we cannot exclude the possibility that some participants in the normal study population had undiagnosed coronary artery or other cardiac diseases. However, a possible effect of these conditions on the heart structure is unlikely to be significant in the context of our study. Fifth, the artefact-based approach presented in our study requires further evaluation. Sixth, the description of the curve artefacts is a subjective approach, which needs comparison to independent noise detection. In the near future, the authors intend to correlate automatically detected 2D grey-scale imaging artefacts with curve-artefacts for further validation. Finally, the Russian population did not include APLAX views in their echocardiograms, and strain-analysis was only performed on 21% of the APLAX views of the Tromsø population. However, APLAX segments in the Tromsø7 population showed the same range of values as the 4-CH view, and the inclusion or exclusion of APLAX segments did not change the results of the segmental values in samples from Tromsø7.

### Clinical implications

Our results showed that the presence of curve artefacts lowers segmental systolic S/SR values, regardless of segment localisation. Because of their similarity to pathology, these artefacts must be identified to avoid misinterpretation of the biased low values as evidence of regionally reduced heart function. In contrast, foreshortening artefacts systematically increased S/SR values, which did not change the interpretation of the presence or absence of pathologies during clinical examination. Pathologically reduced strain curves have a curve with reduced segmental peak strain is followed by PSS, and after the PSS peak, all segments display parallel stretching at the end of the early diastolic and atrial filling phases.

In this study, we described an approach for defining strain-curve artefacts using subjective visual assessment.

If this subjective approach is robust as compared with objective 2D imaging artefact detection, curve artefact algorithms can potentially be integrated into automated reading programmes. Timely manual or automated detection of artificial curve shapes facilitates the correct interpretation of strain results without repeated assessment of tracking. Finally, during real-time strain recordings, curve artefact detection might be performed to provide immediate feedback on imaging quality. Other algorithms can be developed taking both, curve artefacts, noise, reverberations, or missing segments into account to help reconstruct discarded segments on the base of the ventricular shape, size and strain curves of artefact-free segments.

### CONCLUSIONS

Strain-curve artefacts introduce systematic errors, resulting in reduced segmental S/SR values. In contrast to the rather robust GLS, the recognition of curve artefacts is crucial for the correct interpretation of segmental S/SR patterns. Segmental S/SR in a normal population showed substantial gradients, increasing from the epicardial to endocardial position and basal-septal towards apical segments. Inter-segmental S/SR gradients and artefacts should be considered for the correct definition of normalcy and pathology.

### Author affiliations

<sup>1</sup>Department of Clinical Medicine, UiT The Arctic University, Tromsø, Norway

<sup>2</sup>Department of Cardiology, Division of Cardiothoracic and Respiratory Medicine, University Hospital of North Norway, Tromsø, Norway

<sup>3</sup>International Research Competence Center, Northern State Medical University of the Ministry of Health of the Russian Federation, Arhangel'sk, Russian Federation

<sup>4</sup>Research Institute of Internal and Preventive Medicine, Novosibirsk Science Center of the Siberian Branch of the Russian Academy of Sciences, Novosibirsk, Russian Federation

<sup>5</sup>Department of Non-invasive Diagnostics, Novosibirsk State Medical University, Novosibirsk, Russian Federation, Novosibirsk, Russian Federation

<sup>6</sup>Department of Community Medicine, UiT The Arctic University of Norway, Tromsø, Norway

<sup>7</sup>Department of Cardiology, Akershus Universitetssykehus HF, Lorenskog, Norway

**Acknowledgements** We would like to acknowledge the contribution of the KYH and Tromsø7 study participants. Further, we would like to thank Editage ([www.editage.com](http://www.editage.com)) for English language editing.

**Contributors** MK: data collection, strain analysis, statistical analysis and writing of the manuscript; HAC: artefact analysis, strain analysis for the interobserver variability; AK: data collection in Arkhangelsk, writing of the manuscript; SM and AnR funding acquisition and data collection in Novosibirsk, writing of the manuscript; MS, conventional echocardiographic measurements, writing of the manuscript; HS: design funding and conduction of the Tromsø7 study and writing of the manuscript; AsR: introduction of the new concept of curve-artefacts, study design, guarantor, funding of the PhD project, statistical analyses and writing of the manuscript.

**Funding** This KYH study was a component of the International Project on CVD in Russia (IPCDR). The IPCDR was funded by the Wellcome Trust Strategic Award (No. 100 217) and supported by funds from UiT, The Arctic University of Norway, Norwegian Institute of Public Health, and the Norwegian Ministry of Health and Social Affairs. SM was supported by the Russian Academy of Science, State target

(#122031700094-5). The first author received a PhD grant from Helse Nord RHF (HNF 1458-19).

**Disclaimer** The study sponsor/funder was not involved in the design of the study; the collection, analysis, and interpretation of data; writing the report; and no restrictions were imposed regarding the publication of the report.

**Competing interests** None declared.

**Patient consent for publication** Consent obtained directly from patient(s).

**Ethics approval** Beyond the approval for the conduction of the Tromsø7 and Know Your Heart study, the study received an ethical approval of the Regional Ethical Committee (reference number: #REK Nord 45140). The study complies with the Declaration of Helsinki. An informed consent was obtained by all study subjects.

**Provenance and peer review** Not commissioned; externally peer reviewed.

**Data availability statement** Data relevant to this study can be made available on reasonable request to the corresponding author.

**Supplemental material** This content has been supplied by the author(s). It has not been vetted by BMJ Publishing Group Limited (BMJ) and may not have been peer-reviewed. Any opinions or recommendations discussed are solely those of the author(s) and are not endorsed by BMJ. BMJ disclaims all liability and responsibility arising from any reliance placed on the content. Where the content includes any translated material, BMJ does not warrant the accuracy and reliability of the translations (including but not limited to local regulations, clinical guidelines, terminology, drug names and drug dosages), and is not responsible for any error and/or omissions arising from translation and adaptation or otherwise.

**Open access** This is an open access article distributed in accordance with the Creative Commons Attribution Non Commercial (CC BY-NC 4.0) license, which permits others to distribute, remix, adapt, build upon this work non-commercially, and license their derivative works on different terms, provided the original work is properly cited, appropriate credit is given, any changes made indicated, and the use is non-commercial. See: <http://creativecommons.org/licenses/by-nc/4.0/>.

#### ORCID iDs

Andrew Ryabikov <http://orcid.org/0000-0001-9868-855X>

Henrik Schirmer <http://orcid.org/0000-0002-9348-3149>

Assami Rösner <http://orcid.org/0000-0001-9084-5805>

#### REFERENCES

- Marwick TH, Leano RL, Brown J, *et al*. Myocardial strain measurement with 2-Dimensional speckle-tracking echocardiography: definition of normal range. *JACC Cardiovasc Imaging* 2009;2:80–4.
- Kalam K, Otahal P, Marwick TH. Prognostic implications of global LV dysfunction: a systematic review and meta-analysis of global longitudinal strain and ejection fraction. *Heart* 2014;100:1673–80.
- Mor-Avi V, Lang RM, Badano LP, *et al*. Current and evolving echocardiographic techniques for the quantitative evaluation of cardiac mechanics: ASE/EAE consensus statement on methodology and indications endorsed by the Japanese Society of echocardiography. *J Am Soc Echocardiogr* 2011;24:277–313.
- Perk G, Tunick PA, Kronzon I. Non-Doppler two-dimensional strain imaging by echocardiography—from technical considerations to clinical applications. *J Am Soc Echocardiogr* 2007;20:234–43.
- Marwick TH. Measurement of strain and strain rate by echocardiography: ready for prime time? *J Am Coll Cardiol* 2006;47:1313–27.
- Kim S-A, Park S-M, Kim M-N, *et al*. Assessment of left ventricular function by Layer-Specific strain and its relationship to structural remodelling in patients with hypertension. *Can J Cardiol* 2016;32:211–6.
- Sarvari SI, Haugaa KH, Zahid W, *et al*. Layer-specific quantification of myocardial deformation by strain echocardiography may reveal significant CAD in patients with non-ST-segment elevation acute coronary syndrome. *JACC Cardiovasc Imaging* 2013;6:535–44.
- Tarascio M, Leo LA, Klersy C, *et al*. Speckle-Tracking Layer-Specific analysis of myocardial deformation and evaluation of scar Transmurality in chronic ischemic heart disease. *J Am Soc Echocardiogr* 2017;30:667–75.
- Ünlü S, Mirea O, Pagourelis ED, *et al*. Layer-Specific segmental longitudinal strain measurements: capability of detecting myocardial scar and differences in feasibility, accuracy, and reproducibility, among four vendors a report from the EACVI-ASE strain standardization Task force. *J Am Soc Echocardiogr* 2019;32:e11:624–32.
- Leitman M, Lysyansky P, Sidenko S, *et al*. Two-Dimensional strain—a novel software for real-time quantitative echocardiographic assessment of myocardial function. *J Am Soc Echocardiogr* 2004;17:1021–9.
- Nagata Y, Wu VC-C, Otsuji Y, *et al*. Normal range of myocardial layer-specific strain using two-dimensional speckle tracking echocardiography. *PLoS One* 2017;12:e0180584.
- Sugimoto T, Dulgheru R, Bernard A, *et al*. Echocardiographic reference ranges for normal left ventricular 2D strain: results from the EACVI NORRE study. *Eur Heart J Cardiovasc Imaging* 2017;18:833–40.
- Ünlü S, Duchenne J, Mirea O, *et al*. Impact of apical foreshortening on deformation measurements: a report from the EACVI-ASE strain standardization Task force. *Eur Heart J Cardiovasc Imaging* 2020;21:337–43.
- Alcidi GM, Esposito R, Evola V, *et al*. Normal reference values of multilayer longitudinal strain according to age decades in a healthy population: a single-centre experience. *Eur Heart J Cardiovasc Imaging* 2018;19:1390–6.
- Dalen H, Thorstensen A, Aase SA, *et al*. Segmental and global longitudinal strain and strain rate based on echocardiography of 1266 healthy individuals: the HUNT study in Norway. *Eur J Echocardiogr* 2010;11:176–83.
- Kuznetsova T, Herbots L, Richart T, *et al*. Left ventricular strain and strain rate in a general population. *Eur Heart J* 2008;29:2014–23.
- Tsugu T, Postolache A, Dulgheru R, *et al*. Echocardiographic reference ranges for normal left ventricular layer-specific strain: results from the EACVI NORRE study. *Eur Heart J Cardiovasc Imaging* 2020;21:896–905.
- Yingchoncharoen T, Agarwal S, Popović ZB, *et al*. Normal ranges of left ventricular strain: a meta-analysis. *J Am Soc Echocardiogr* 2013;26:185–91.
- Kocabay G, Muraru D, Peluso D, *et al*. Normal left ventricular mechanics by two-dimensional speckle-tracking echocardiography: reference values in healthy adults. *Rev Esp Cardiol* 2014;67:651–8.
- Poulsen SH, Andersen NH, Ivarsen PI, *et al*. Doppler tissue imaging reveals systolic dysfunction in patients with hypertension and apparent "isolated" diastolic dysfunction. *J Am Soc Echocardiogr* 2003;16:724–31.
- Hurlburt HM, Aurigemma GP, Hill JC, *et al*. Direct ultrasound measurement of longitudinal, circumferential, and radial strain using 2-Dimensional strain imaging in normal adults. *Echocardiography* 2007;24:723–31.
- Reckefuss N, Butz T, Horstkotte D, *et al*. Evaluation of longitudinal and radial left ventricular function by two-dimensional speckle-tracking echocardiography in a large cohort of normal probands. *Int J Cardiovasc Imaging* 2011;27:515–26.
- Guseva VP, Ryabikov AN, Voronina EV, *et al*. [The changes of left ventricular longitudinal systolic function depending on hypertension and its control: analysis in a population]. *Kardiologiya* 2020;60:36–43.
- Menting ME, McGhie JS, Koopman LP, *et al*. Normal myocardial strain values using 2D speckle tracking echocardiography in healthy adults aged 20 to 72 years. *Echocardiography* 2016;33:1665–75.
- Sun JP, Lee AP-W, Wu C, *et al*. Quantification of left ventricular regional myocardial function using two-dimensional speckle tracking echocardiography in healthy volunteers—a multi-center study. *Int J Cardiol* 2013;167:495–501.